Increasing the Reactivity of an Artificial Dithiol−Disulfide Pair through Modification of the Electrostatic Milieu

Rosa E. Hansen,[‡] Henrik Østergaard,[§] and Jakob R. Winther*,[‡]

Carlsberg Laboratory, Gamle Carlsberg Vej 10, DK-2500 Copenhagen Valby, Denmark

Received January 7, 2005; Revised Manuscript Received February 11, 2005

ABSTRACT: The thiol−disulfide exchange reaction plays a central role in the formation of disulfide bonds in newly synthesized proteins and is involved in many aspects of cellular metabolism. Because the thiolate form of the cysteine residue is the key reactive species, its electrostatic milieu is thought to play a key role in determining the rates of thiol disulfide exchange reactions. While modest reactivity effects have previously been seen in peptide model studies, here, we show that introduction of positive charges can have dramatic effects on disulfide bond formation on a structurally restricted surface. We have studied properties of vicinal cysteine residues in proteins using a model system based on redox-sensitive yellow fluorescent protein (rxYFP). In this system, the formation of a disulfide bond between two cysteines Cys149 and Cys202 is accompanied by a 2.2-fold decrease in fluorescence. Introduction of positively charged amino acids in the proximity of the two cysteines resulted in an up to 13-fold increase in reactivity toward glutathione disulfide. Determination of the individual pK_a values of the cysteines showed that the observed increase in reactivity was caused by a decrease in the pK_a value of Cys149, as well as favorable electrostatic interactions with the negatively charged reagents. The results presented here show that the electrostatic milieu of cysteine thiols in proteins can have substantial effects on the rates of the thiol−disulfide exchange reactions.

Two fundamental properties characterize vicinal thiol−disulfide pairs in proteins and in organic compounds in general: reactivity and redox potential. These properties are of particular importance for the function of redox-active enzymes and have been studied extensively. The best-characterized enzymes in this group are the thiol−disulfide oxidoreductases belonging to the thioredoxin family (*1*, *2*). These all contain the Cys−X−X−Cys active-site motif and include enzymes both involved in reduction of disulfide bonds (like thioredoxin) and enzymes that are primarily protein thiol oxidases, like DsbA or protein disulfide isomerase. Although enzymes of this class have been subjected to extensive biochemical characterization, the features that dictate their reactivity and redox potentials are not fully understood. While there are numerous examples of mutations in such proteins aimed at changing redox potential (*3*−*5*), mutagenesis strategies have mostly been governed by homology considerations. Because these enzymes are highly specialized, the reactivity and redox potential of the active-site thiols involve a complex combination of electrostatic properties and various degrees of structural strain. At the other end of the complexity scale are careful characterizations of model peptides containing cysteine residues in various sequence contexts (*6*). However, such compounds are normally highly flexible and generally mimic the ordered structure of proteins poorly.

Therefore, while thiol−disulfide redox processes have been the focus of much research, there are only few examples of model proteins where thiol−disulfide equilibrium and reactivity are easily assayed and at the same time offer tractable possibilities for manipulation. We have previously engineered an exposed disulfide bond into the yellow fluorescent variant of the green fluorescent protein (rxYFP, ref *7*). The cysteines forming the bond were introduced at positions 149 and 202, connecting adjacent β strands that make up part of the rigid scaffold surrounding the central fluorophore of the protein. The introduced disulfide bond is unique in several ways: (a) it is readily accessible to added oxidants and reductants such as the physiological relevant glutathione (GSH)[1] and glutathione disulfide (GSSG); (b)

* To whom correspondence should be addressed: Institute of Molecular Biology and Physiology, University of Copenhagen, Universitetsparken 13, DK-2100 Copenhagen, Denmark. Telephone: +45 3532 1500. Fax: +45 3532 1567. E-mail: jrwinther@aki.ku.dk.

‡ Present address: Institute of Molecular Biology and Physiology, University of Copenhagen, Universitetsparken 13, DK-2100 Copenhagen, Denmark.

§ Present address: Novo Nordisk A/S, Novo Nordisk Park, DK-2760 Måløv, Denmark.

[1] Abbreviations: CHES, cyclohexylaminoethane sulfonic acid; DTT, dithiothreitol; EDTA, ethylenediaminetetraacetic acid; f_{SH}, fraction of unmodified scrxYFP; GFP, green fluorescent protein; GSH, glutathione; GSSG, glutathione disulfide; HED, 2-hydroxyethyldisulfide; HEPES, (*N*-[2-hydroxyethyl]piperazine-*N*′-[2-ethanesulfonic acid]); IAA, iodoacetic acid; IAM, iodoacetamide; k_{app}, apparent second-order rate constant; k', pseudo first-order rate constant; k_{max}, limiting rate constant; MES, 2-(*N*-morpholino)ethanesulfonic acid; NEM, *N*-ethylmaleimide; PAGE, polyacrylamide gel electrophoresis; rxYFP, redox-sensitive yellow fluorescent protein; scrxYFP, single-cysteine rxYFP; $scrxYFP_{SH}$, unmodified single-cysteine rxYFP; $scrxYFP_{SSG}$, glutathionylated single-cysteine rxYFP; $scrxYFP_{SAA}$, IAA-modified single-cysteine rxYFP; Tris, tris(hydroxymethyl)aminomethane; YFP, yellow fluorescent protein; wt, wild type.

10.1021/bi0500372 CCC: $30.25
Published on Web 03/19/2005

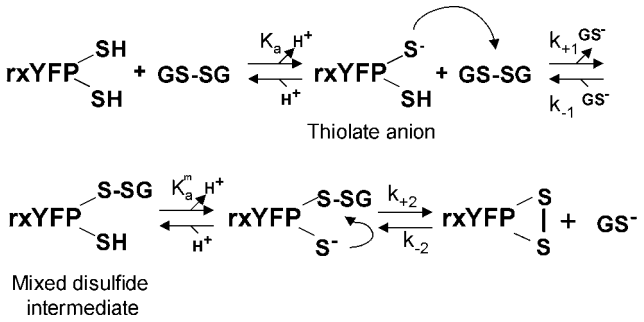

FIGURE 1: Mechanism of thiol−disulfide exchange between rxYFP and GSSG. The thiolate anion is the reactive nucleophile in thiol−disulfide exchange reactions. The mixed disulfide intermediate is formed by the nucleophilic attack of the rxYFP thiolate anion on the disulfide bond of GSSG resulting in the release of one molecule of GS^-. Subsequently, an intramolecular nucleophilic attack on the mixed disulfide by the second cysteine in rxYFP leads to the formation of the intramolecular disulfide and the release of another GSH molecule. Stabilization of the $rxYFP_{SH}^{S-}$ thiolate makes it a better leaving group. k_{+1}, k_{-1}, k_{+2}, and k_{-2} are the respective rate constants. K_a and K_a^m denote the acid dissociation constant for the reactive cysteine thiol and the cysteine thiol in the mixed disulfide intermediate, respectively.

its thermodynamic stability and reactivity toward such low-molecular-weight thiol−disulfides are within easily measurable ranges; and (c) its formation reduces the fluorescence signal from YFP by 2.2-fold (at neutral pH). This construct constitutes a structurally well-defined system in which the two cysteine residues are located on a rigid platform on which adjacent amino acid residues may be altered to affect the reactivity and redox potential of the cysteine pair.

Thiol−disulfide exchange reactions take place via an S_N2 mechanism in which the thiolate anion is the reactive nucleophile (*8*). This enables formation of the mixed disulfide intermediate (Figure 1). In the case of vicinal thiols (like in rxYFP), subsequent formation of the intramolecular disulfide bond is expected to be very rapid ($k_{+2} \gg k_{+1}$ [GSSG]; Figure 1). Thus, the initial step is rate limiting, and the observed rate constant depends on the fraction of thiol present as the anion. Accordingly, factors affecting the pK_a of the nucleophilic thiol, e.g., introduction of charged residues in proximity of the redox-active cysteines, should result in an altered reaction rate.

To gauge the potential magnitude of such effects in a well-defined system, we have studied the effect of introducing positively charged amino acid residues at positions that were expected to influence the disulfide bond in rxYFP. We find that such mutations strongly increase the reactivity toward GSSG. We also show that Cys149 acts as the predominant thiolate and that the increased reactivity is caused by a combination of favorable electrostatic interactions and a stabilization of the predominant thiolate.

EXPERIMENTAL PROCEDURES

Site-Directed Mutagenesis of rxYFP. Mutations were introduced into the *rxYFP* gene using QuickChange site-directed mutagenesis (Stratagene) on pHOJ100 (lacking redox-active Cys residues) or pHOJ124 [encoding rxYFP (*7*)]. The coding sequence of the latter plasmid defines the term "wt rxYFP" as used in the present paper. Forward primers are listed in Table 1. To facilitate subsequent screening of transformants for successful incorporation of mutations, all primers included silent mutations introducing unique restriction sites. All variants were confirmed by sequence analysis of the entire gene.

Expression and Purification of Proteins. Proteins were expressed in *Escherichia coli* strain BL21(DE3) (Novagen) by use of the pET24 expression system (Novagen). Cultures were grown at 37 °C in Terrific Broth with 30 μg/mL kanamycin (*9*). At an OD_{600} of 1.5, the growth temperature was shifted to 18 °C and protein expression was induced by the addition of isopropyl-β-D-thiogalactopyranoside (Sigma) to 0.25 mM. After 17 h of incubation, the cells were harvested and lysed as described (*7*). Lysates of the single-cysteine rxYFP variants were precipitated by addition of ammonium sulfate to 82% saturation. After centrifugation, the pellets were resuspended in water and desalted on a Sephadex G-25 (Amersham Pharmacia Biotech) column equilibrated with 25 mM potassium phosphate at pH 7.2. Finally, the protein was subjected to anion-exchange chromatography on a 6 mL Resource Q column (Amersham Pharmacia Biotech) equilibrated with 25 mM potassium phosphate at pH 7.0. Proteins were eluted with a gradient of KCl (0−0.15 M) in 25 mM potassium phosphate at pH 7.0 over 40 min at a flow rate of 2 mL/min. The proteins were estimated to be >95% pure as judged by SDS−PAGE.

Purification of the rxYFP arginine variants was carried out by loading the lysates onto a DE52 (Whatman) anion-exchange column equilibrated in 5 mM potassium phosphate at pH 7.0. After the wash, the proteins were batch-eluted with 5 mM potassium phosphate at pH 7.0 containing 1 M

Table 1: Oligonucleotides Used for Mutagenesis

resulting plasmid	template plasmid	primer 5′−3′
pHOJ173 ($scrxYFP_{149C}$)	pHOJ100	CCG GTG CTG CTG CCG GAC AAC CAT TAC CTG TGC TAC CAG TCT GCC
pHOJ172 ($scrxYFP_{202C}$)	pHOJ104	CCG GTG CTG CTG CCG GAC AAC CAT TAC CTG TCC TAC CAG TCT GCC
pRH5 ($scrxYFP_{149C}^{200R}$)	pHOJ100	CCG GTG CTG CTG CCG GAC AAC CAC CGG TTG TGC TAC CAG TCT GCC
pRH15 ($scrxYFP_{202C}^{200R}$)	pHOJ104	CCG GTG CTG CTG CCG GAC AAC CAT CGA TTG TCC TAC CAG TCT GCC
pRH24 ($scrxYFP_{149C}^{227R}$)	pHOJ173	G CTG GAA TTT GTG ACC GCC CGC GGC ATC ACG CAT GGC
pRH18 ($rxYFP^{204R}$)	pHOJ104	G CTG CTG CCG GAC AAC CAT AAG CTT TGC TAC CAG TCT GCC CTT TCG
pRH17 ($rxYFP^{227R}$)	pHOJ104	G CTG GAA TTT GTG ACC GCC CGC GGC ATC ACG CAT GGC
pHOJ120 ($rxYFP^{200R}$)	pHOJ104	C AAC CAT CGC CAG TGC TAC CAG TCT GCC CTT TCG AAA GAT CCG
pRH20 ($rxYFP^{200R/204R}$)	pHOJ104	G GTG CTG CTG CCG GAC AAC CAT CGG CTG TGC TAC CGG TCT GCC CTT TCG
pRH21 ($rxYFP^{200R/227R}$)	pHOJ120	G CTG GAA TTT GTG ACC GCC CGC GGC ATC ACG CAT GGC
pRH22 ($rxYFP^{204R/227R}$)	pRH17	G CTG CTG CCG GAC AAC CAT AAG CTT TGC TAC CAG TCT GCC CTT TCG
pRH23 ($rxYFP^{200R/204R/227R}$)	pRH20	G CTG GAA TTT GTG ACC GCC CGC GGC ATC ACG CAT GGC

KCl. Although this procedure did not result in pure protein preparations, control experiments verified that the contaminants did not influence the subsequent characterization of the variants.

Analytical Techniques. Protein concentration was determined using the known extinction coefficient (ϵ) of the base-denatured chromophore at 447 nm ($\epsilon_{447nm} = 44\,000$ M^{-1} cm^{-1}) as described (*10*). Thiol concentrations [GSH and dithiothreithol (DTT), Sigma] in stock solutions were determined in a 0.1 M potassium phosphate buffer at pH 7.0, using Ellman's reagent [5,5′-dithiobis(2-nitrobenzoic acid)]. The molar extinction coefficient of 14 150 M^{-1} cm^{-1} of 2-nitro-5-thiobenzoic acid at 412 nm was used (*11*). Stock solutions of GSSG (Calbiochem) were quantified from their absorbance at 248 nm [$\epsilon = 382$ M^{-1} cm^{-1}, (*12*)]. Prior to all experiments, the pH of GSH and GSSG stock solutions was adjusted to 7.0 using KOH. Concentrations of iodoacetic acid (IAA) and iodoacetamide (IAM, Sigma) were determined by comparing the thiol concentration of a slight excess of DTT before and after treatment with the alkylating agent. All concentrations were determined by three independent measurements. Preparation of reduced rxYFP was performed as described (*13*).

Fluorescence Measurements. Fluorescence measurements were performed using a Perkin−Elmer Luminescence Spectrometer LS50B with a thermostated, stirred single-cell holder. Excitation and emission wavelengths were 512 and 523 nm, respectively, at 3 nm slit widths. All measurements were carried out in 100 mM potassium phosphate at pH 7.0 and 1 mM EDTA at 30 °C. Prior to all experiments, buffers were thoroughly purged with argon to prevent interference from dissolved molecular oxygen. The fluorescence properties of the arginine mutants were similar to those of wt rxYFP with excitation and emission peaks at 512 and 523 nm, respectively. However, the relative fluorescence changes upon oxidation/reduction were slightly smaller, from 1.8- to 2.1-fold as compared to 2.2-fold for rxYFP (data not shown).

Rate Constant for the Oxidation of Reduced rxYFP. Apparent second-order rate constants (k_{app}) for the reactions between reduced rxYFP variants and GSSG, 2-hydroxyethyldisulfide (HED, Sigma), or cysteamine disulfide (Fluka) were determined by following the decrease in fluorescence at 523 nm (*13*). Reactions were performed at 30 °C in 100 mM potassium phosphate at pH 7.0 containing 1 mM EDTA. Proteins were diluted to ∼0.2 μM in 2 mL of prewarmed buffer. When a stable baseline was attained, the reaction was initiated by the addition of a high molar excess of oxidizing agent to ensure pseudo first-order conditions. Pseudo-first-order rate constants were determined by fitting the progress curves to a single-exponential function. A minimum of six independent measurements was performed at varying concentrations of oxidizing agent. The apparent second-order rate constants were then obtained by a linear fit to the estimated pseudo first-order rate constants.

pK_a Determinations. Individual pK_a values of the cysteines in wt rxYFP and the cysteines in the rxYFP variant where position 200 was mutated to arginine ($rxYFP^{200R}$) were determined using the corresponding single-cysteine variants, denoted scrxYFP. To ensure that the thiol group in the variants was accessible to modification, proteins were pretreated with DTT as described previously (*13*). The rates of carboxymethylation of the scrxYFP's were determined by incubating the reduced proteins (∼3 μM) with a large excess of IAA in a buffer mixture consisting of 10 mM MES, 10 mM HEPES, 10 mM CHES, and 0.1 M Na_2SO_4 at pH values ranging from 7 to 10. After various times of incubation, the reactions were quenched by the addition of 20 mM DTT. All reactions were carried out at 30 °C. Because of differences in reactivity, experiments with wt scrxYFP's were carried out using 1.35 mM IAA, while only 88 μM IAA was used for the 200R variants. In all cases, the observed reaction kinetics fitted well to a single-exponential decay function consistent with pseudo first-order conditions. Reduced and IAA-modified scrxYFP's were separated on nondenaturing 10% polyacrylamide gels in Tris-glycine buffer at pH 8.3, run at 100 V for 2 h. The gel-loading buffer contained 20% glycerol and 0.2% bromophenol blue. Bands on the gels were detected using a Storm Phosphorimager scanner and quantified using ImageQuant software (Molecular Dynamics). The observed pH-dependent reaction rate constants were fitted to the Henderson−Hasselbalch equation using Kaleidagraph (Synergy Software): $k' = k'_{max}/[1 + 10^{(pKa-pH)}]$. Here, k'_{max} represents the limiting rate constant at high pH.

Alkylation of scrxYFP Variants with IAM. Alkylation reactions were performed essentially as described above, but in these experiments, reduced scrxYFP's were blocked with IAM and IAA was used as a quenching agent. Because IAM carries no charge, IAA- and IAM-modified proteins can be separated by nondenaturing gel electrophoresis. Concentrations of 0.7 and 0.16 mM IAM were used for the experiments with scrxYFP and its mutant forms, respectively. All reactions were quenched with 2.7 mM IAA.

Determination of K_{scox}. Equilibrium constants (K_{scox}) for the reaction between scrxYFP and glutathione were determined by incubation of ∼3 μM protein in 100 mM potassium phosphate at pH 7.0 and 1 mM EDTA containing varying concentrations of GSH (1−20 mM) and GSSG (0.1−10 mM). After equilibration of the samples under argon atmosphere for 3 h at 30 °C, the reactions were quenched by alkylating the free thiols by addition of 32 mM IAM. *N*-ethylmaleimide (NEM) was also tested as a quenching agent. However, this compound could not be used because of nonspecific modification of other residues.

Free (IAM-modified) and glutathionylated proteins were separated and quantified by nondenaturing gel electrophoresis as described above. K_{scox} values were estimated from the relationship

$$f_{SH} = ([GSH]/[GSSG])/(K_{scox} + [GSH]/[GSSG])$$

where f_{SH} is the fraction of nonglutathionylated scrxYFP. Because of air oxidation and GSSG contamination in the GSH stock, the exact amount of GSSG in the redox reaction was determined by HPLC essentially as described (*14*).

RESULTS

Increasing the Reactivity of rxYFP toward Glutathione. We based the selection of relevant sites for introduction of positively charged amino acid residues in rxYFP on visual inspection of the crystal structure of the oxidized form of the protein (*7*). This approach resulted in identification of three solvent-exposed residues, Tyr200, Gln204, and Ala227, respectively, that were within a distance of the redox-active

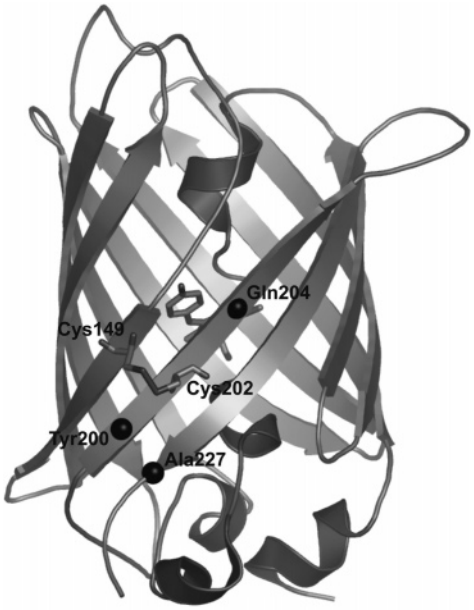

FIGURE 2: Crystal structure of the oxidized form of rxYFP. The C_α positions of Tyr200, Gln204, and Ala227, investigated in the present work, are marked by black spheres. The distances between the C_α atoms and the closest sulfur atom in the disulfide bond were measured to 5.3 Å for Y200−C202, 8.9 Å for Q204−C149, and 5.8 Å for A227−C202, respectively. The chromophore and the Cys149−Cys202 disulfide are shown as ball-and-stick representations. The figure was drawn using PyMOL (http://www.pymol.org) on atomic coordinates obtained from 1H6R from the Protein Data Bank.

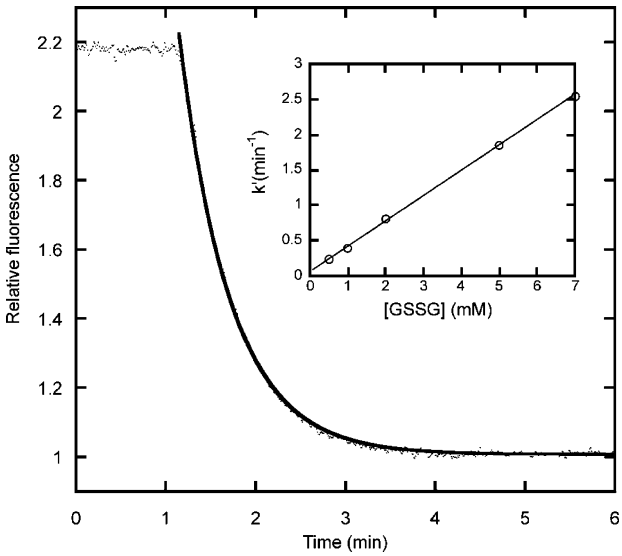

FIGURE 3: Determination of rate constants for the reaction between $rxYFP^{200R}$ and GSSG. The reaction between $rxYFP^{200R}$ (~2 μM) and GSSG was performed under pseudo first-order conditions with 5 mM GSSG in 100 mM potassium phosphate at pH 7.0 and 1 mM EDTA at 30 °C. The reaction was followed by a change in fluorescence at 523 nm upon excitation at 512 nm. A pseudo first-order rate constant $k' = 1.80 \pm 0.006$ min^{-1} was obtained by fitting the progress curve to a single-exponential function. (Inset) Plot of k' versus [GSSG], obtained from a series of similar experiments with varying GSSG concentrations, yielded a value of 370 ± 5.7 M^{-1} min^{-1} for the apparent second-order rate constant. The relative second-order rate constants for the remaining rxYFP variants are shown in Figure 4.

cysteines that made them obvious candidates for introduction of positive charges (Figure 2). Each of these residues was mutated to either arginine or lysine.

The reactivities toward oxidized glutathione were based on the observation that formation of a disulfide bond in rxYFP results in an about 2-fold decrease in fluorescence at 523 nm. Apparent second-order rate constants (k_{app}) were determined from a series of reactions performed under pseudo first-order conditions with a $>10^3$-fold molar excess of GSSG (Figure 3). As shown in Figure 4A, k_{app} had increased in all mutants and in all positions arginine had a larger effect on reactivity than lysine. The most reactive variant, $rxYFP^{200R}$, was 5.2-fold more reactive than wt rxYFP.

The possibility that introduction of two positive charges would have a larger effect on the reactivity than introduction of one prompted us to prepare variants where arginine residues were introduced in all combinations at the three positions. The reactivity toward glutathione was determined as described, and the results are shown in Figure 4B. Introduction of several positive charges indeed increased the reactivity toward GSSG further, with the most reactive mutant being the triple mutant with a 13-fold increased k_{app} relative to rxYFP.

Because glutathione has an overall negative charge between −1 and −2 at pH 7, we hypothesized that part of the increase in reactivity could be due to electrostatic interactions with glutathione. To test this, we measured the rate of rxYFP oxidation by the noncharged disulfide HED (the disulfide form of 2-mercaptoethanol) as well as the positively charged cysteamine disulfide. Figure 4B shows a comparison of the rate constants, normalized to one for wt. In comparison to wt rxYFP, the reaction rates with all three oxidizing agents were increased for all mutants. However, the arginine substitutions appeared to strongly favor the reaction with GSSG. This is most evident for the triple mutant, where a 13-fold increase in the rate constant was observed for the reaction with the negatively charged glutathione, while the increase was only 4.3-fold for the reaction with HED and 2.1-fold for the reaction with the positively charged cysteamine disulfide. The substantial electrostatic contribution to the reaction with GSSG for this mutant was confirmed by comparing the rates of oxidation of wt rxYFP and $rxYFP^{200R/204R/227R}$ by 5 mM GSSG at different ionic strengths in a pH 7 buffer supplemented with 0−160 mM K_2SO_4 (Figure 5). While the reaction rate of wt rxYFP was nearly independent of the ionic strength, the rate constant of the triple arginine mutant decreased as the salt concentration increased.

Determination of Redox-Active Cysteine pK_a Values. Because our data suggested that the introduction of positive residues reduced the pK_a value of one or both of the redox-active cysteine residues on rxYFP, we wanted to assess this directly. This was done by preparing and analyzing single-cysteine variants (scrxYFP's) of the redox sensor, where Cys149 or Cys202 were reverted to the amino acid residues originally found in YFP (Asn and Ser, respectively).

The methodology used was based on the following observations: (a) scrxYFP runs as a well-defined band on a 10% nondenaturing polyacrylamide gel; (b) the protein maintains its native structure in the gel and can be detected and quantified by fluorescence scanning; and (c) modification of scrxYFP with negatively charged compounds results in a distinct increase in its electrophoretic mobility. Using this

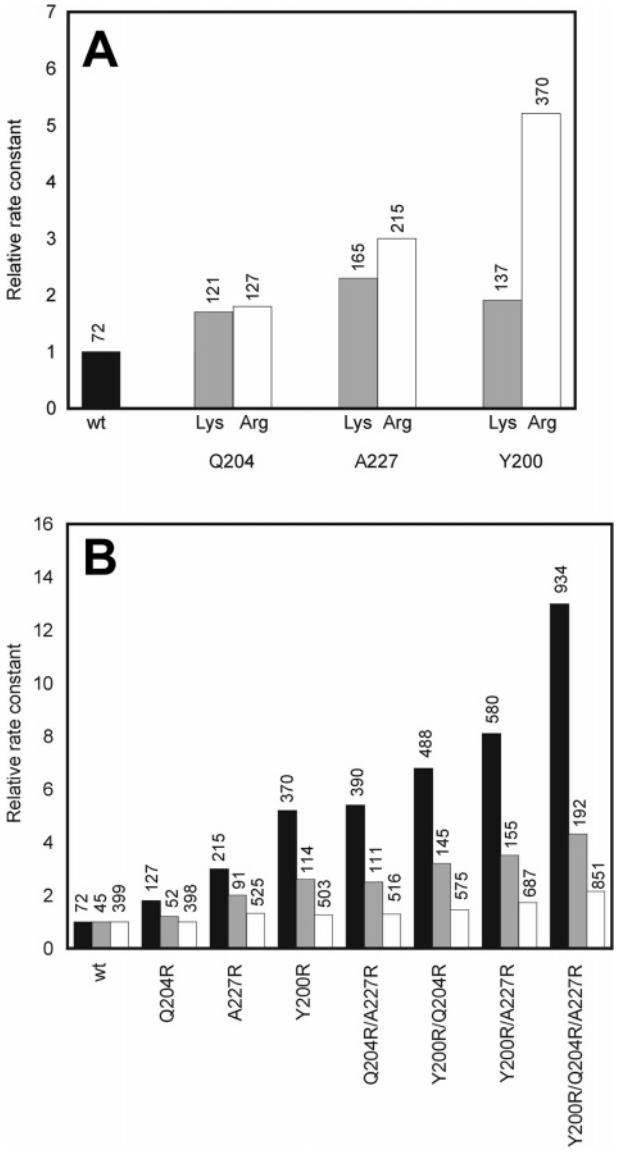

FIGURE 4: Effects of positively charged residues on rxYFP oxidation rates. Apparent second-order rate constants (k_{app}) for all reactions are shown. The graph shows k_{app} values relative to wt rxYFP, which is set to 1, while the absolute values for the rate constants are given above each bar in units of M^{-1} min^{-1}. (A) Lysine (gray bars) and arginine (white bars) residues were introduced at the indicated positions, and k_{app} for the reactions with GSSG are shown relative to wt rxYFP (black bar). (B) Relative k_{app} values for the reaction of rxYFP variants with GSSG (black bars), HED (gray bars), and cystamine disulfide (white bars) are shown. The second-order rate constants were determined as described in Figure 2, and in all cases, the relative standard deviation was less than 5%.

approach, we found the intensity of the bands to be accurately determined within a linear range from 200 ng to 15 μg using a phosphorimager to detect fluorescent bands in the gel (data not shown). Modifications with IAA introduce one negative charge, while modification with glutathione apparently introduces more than one (Figure 6A).

Alkylation of cysteine residues with IAA can take place only if the cysteines are in the thiolate anion state, as shown in reactions 1 and 2 (*15*, *16*). Therefore, measuring the reaction rate as a function of pH can be used to determine the pK_a value of cysteine thiol groups. In the pH range used

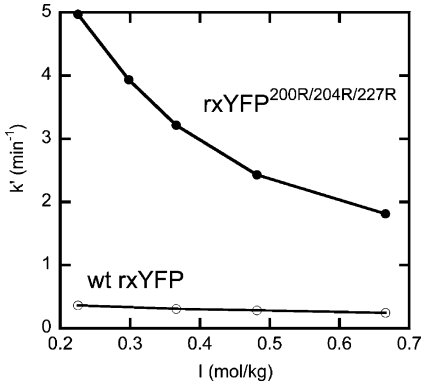

FIGURE 5: Effect of ionic strength on the reactions of wt rxYFP and $rxYFP^{200R/Q204R/227R}$ with 5 mM GSSG. Pseudo first-order rate constants were determined as described in Figure 3 at pH 7.0 and 30 °C in the presence of 100 mM potassium phosphate, 1 mM EDTA, and different K_2SO_4 concentrations ranging from 0 to 160 mM.

in these experiments, IAA does not itself significantly change the ionization state.

$$\text{Cys} - \text{SH} \overset{K_a}{\rightleftharpoons} \text{Cys} - \text{S}^- + \text{H}^+ \quad (1)$$

$$\text{Cys} - \text{S}^- + \text{IAA} \rightarrow \text{Cys} - \text{SAA} + \text{I}^- \quad (2)$$

Pseudo-first-order rate constants for the reaction between the two cysteine variants and a high molar excess of IAA were determined from the band-shift pattern on a nondenaturing gel as exemplified in Figure 6B. Fitting these rate constants in the pH range from 7 to 10 to the Henderson−Hasselbalch equation allowed for an estimation of the pK_a values of Cys149 and Cys202 in rxYFP (Figure 6C). It was found that Cys149 is significantly more reactive at neutral pH, having a pK_a value of 8.90 ± 0.04, than Cys202 with a pK_a of 9.52 ± 0.08. From these results, it can be concluded that Cys149 is the predominant nucleophile at neutral pH.

To investigate the effects of introducing a positive charge in proximity of the reactive cysteine, we compared the pK_a values of Cys149 in $scrxYFP_{149C}$ and $scrxYFP^{200R}_{149C}$ (Figure 6D). pH titrations revealed a decrease in the pK_a of Cys149 from 8.9 to 8.2, implying that part of the increased reactivity results from a stabilization of the reactive redox thiolate. However, in addition to the change in pK_a, a comparison of the titration curves showed that the limiting rate constant (k_{max}) of the reaction with IAA at high pH was 7.6 times larger for the $scrxYFP^{200R}_{149C}$ variant (Figure 6D). Because k_{max} is expected to increase with pK_a according to the Brønsted relationship for small-molecule thiol−disulfide exchange reactions developed by Szajewski and Whitesides (*17*), the further rate enhancement might be explained by an electrostatic effect, where the positive charge of Arg200 attracts the negatively charged IAA.

To test this hypothesis, we applied a variation of the method described for the determination of pK_a values. Here, the scrxYFP's were reacted with IAM for different lengths of time, followed by quenching of the reaction with a large excess of the negatively charged IAA. Because IAM is uncharged, k_{max} should not vary significantly between the wt and mutant protein. The experiment was performed at pH 9, where a 1.6-fold difference between the rate constants of wt $scrxYFP_{149C}$ and $scrxYFP^{200R}_{149C}$ was expected, on the

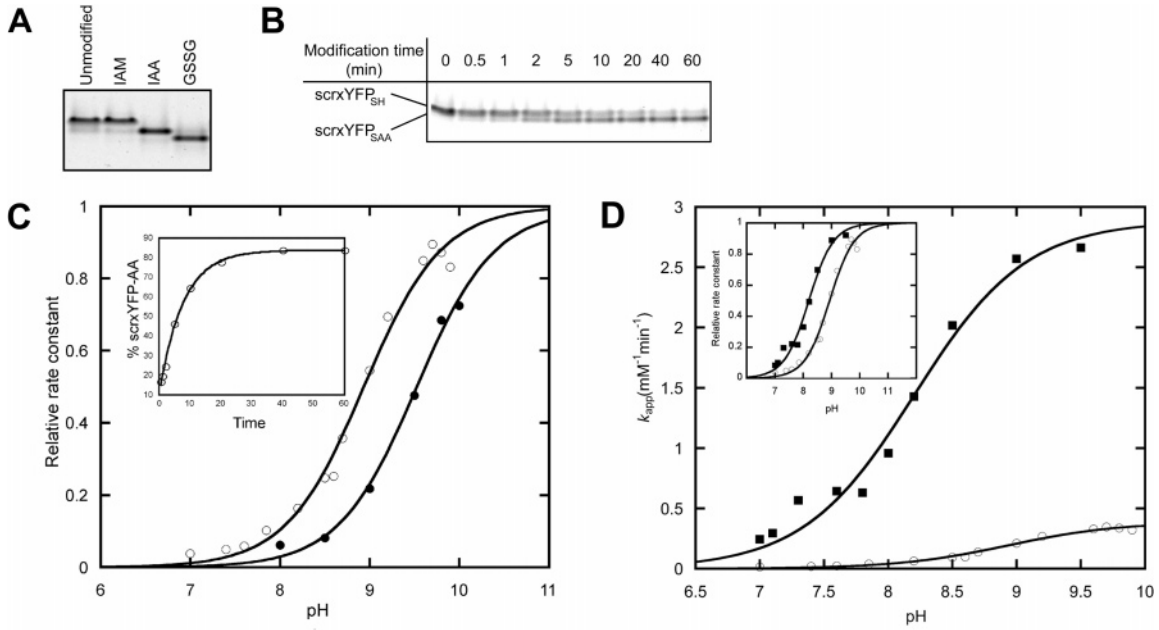

FIGURE 6: Determination of pK_a values using a nondenaturing gel system. (A) Modifications of scrxYFP with negatively charged moieties can be visualized by running samples on a nondenaturing polyacrylamide gel, which separates by charge. Approximately 3 μM *scrxYFP*$^{200R}_{149C}$ was modified with 3 mM iodoacetamide (IAM), 3 mM iodoacetic acid (IAA), or 10 mM GSSG, and samples were loaded onto a 10% polyacrylamide gel. Modification with IAA introduces one charge, and modification with glutathione apparently introduces two, while no changes in mobility take place on modification with the noncharged IAM. (B) Determination of the pseudo first-order rate constant for the reaction between wt scrxYFP$_{149C}$ and IAA at pH 8.5. The reaction between scrxYFP$_{149C}$ and 1.35 mM IAA was quenched with 20 mM DTT at the indicated time points, and 20 μL of the samples were analyzed on a 10% nondenaturing polyacrylamide gel. (C) Relative pseudo first-order rate constants for the reactions of wt scrxYFP$_{149C}$ (○) and wt scrxYFP$_{202C}$ (●) with IAA as a function of pH. Rate constants were determined as described in Figure 3. Data were fitted to the Henderson−Hasselbalch equation (see the Experimental Procedures). The estimated pK_a values are given in the text. (Inset) Using data from B, a pseudo first-order rate constant was determined by fitting the progress curve to a single-exponential function. (D) Comparison of the pH profiles of wt scrxYFP$_{149C}$ (○, as in C) and *scrxYFP*$^{200R}_{149C}$ (■). The pH profiles were obtained as described in C, but the pseudo first-order rate constants have been corrected for differences in IAA concentrations (see the Experimental Procedures) and are therefore depicted as second-order rate constants. Data were fitted to the Henderson−Hasselbalch equation, and the estimated pK_a values are given in the text. The estimated k_{max} values were 0.32 ± 0.04 and 2.90 ± 0.13 mM^{-1} min^{-1} for wt scrxYFP$_{149C}$ and *scrxYFP*$^{200R}_{149C}$, respectively. (Inset) Normalized plot of the pH profiles. At any given pH, the rate enhancements of *scrxYFP*$^{200R}_{149C}$ compared to scrxYFP$_{149C}$ because of the difference in pK_a can be estimated.

basis of the pK_a differences (inset of Figure 6D). The rate constants for the reactions at pH 9 were found to be 0.88 ± 0.14 and 1.51 ± 0.03 mM^{-1} min^{-1} for scrxYFP$_{149C}$ and scrxYFP$^{200R}_{149C}$, respectively. Thus, when reacted with IAM, the rate constant of scrxYFP$^{200R}_{149C}$ was only 1.7 times that of wt, close to the expected value of 1.6. From this, it could be concluded that the difference in k_{max} was caused by attractive electrostatic interactions between IAA and Arg200.

A pH titration of scrxYFP$^{200R}_{202C}$ was also attempted. Unfortunately, the pK_a value of Cys202 in this variant could not be precisely determined, because IAA unspecifically modified other residues at pH above 10 (data not shown). However, the pK_a appeared to have increased compared to scrxYFP$_{202C}$, meaning that the thiolate has been destabilized. Because the attack of Cys202 on the mixed disulfide (Figure 1) is not rate-limiting, this increase in pK_a should not have any effect on the reactivity of rxYFP^{200R}.

Determination of Equilibrium Constants for the Reactions between Glutathione and the scrxYFP Variants. The equilibrium constant, K_{scox}, for the reaction between scrxYFP and glutathione is defined as

$$\text{scrxYFP}_{SH} + \text{GSSG} \rightleftarrows \text{scrxYFP}_{SSG} + \text{GSH}$$

$$K_{scox} = \frac{[\text{scrxYFP}_{SSG}][\text{GSH}]}{[\text{scrxYFP}_{SH}][\text{GSSG}]} \quad (3)$$

The fact that all arginine mutants of rxYFP exhibited increased reactivity toward HED (Figure 4B) suggested that they all exhibited a reduced pK_a of the predominant nucleophile Cys149. This would stabilize the Cys149 thiolate as a leaving group (reaction 3) and thus decrease K_{scox} (*18*). On the other hand, it is conceivable that the same electrostatic interactions that promoted the reaction between scrxYFP and IAA relative to IAM would stabilize the mixed disulfide between scrxYFP and glutathione, leading to an increased K_{scox}. To assess the relative importance of these effects, K_{scox} values for wt and the two arginine mutants were determined. This was done by measuring the ratio between unmodified (scrxYFP$_{SH}$) and glutathionylated (scrxYFP$_{SSG}$) protein at equilibrium in buffers with different concentrations of GSH and GSSG. Equilibrated samples were quenched by a large excess of IAM and analyzed by nondenaturing gel electrophoresis (Figure 7A). K_{scox} values of wt scrxYFP$_{149C}$, scrxYFP$^{227R}_{149C}$, and scrxYFP$^{200R}_{149C}$ were determined to be 5.4 ± 0.4, 3.2 ± 0.2, and 1.30 ± 0.08, respectively (Figure 7B). This suggests that the positive charges stabilize the thiolate of Cys149 as the leaving group (first hypothesis) and that this effect outweighs the interaction between the positive charge of the Arg side chain and the negative charges on GSSG. This stands in contrast to the interaction between Arg and IAA, where the leaving group-effect is irrelevant.

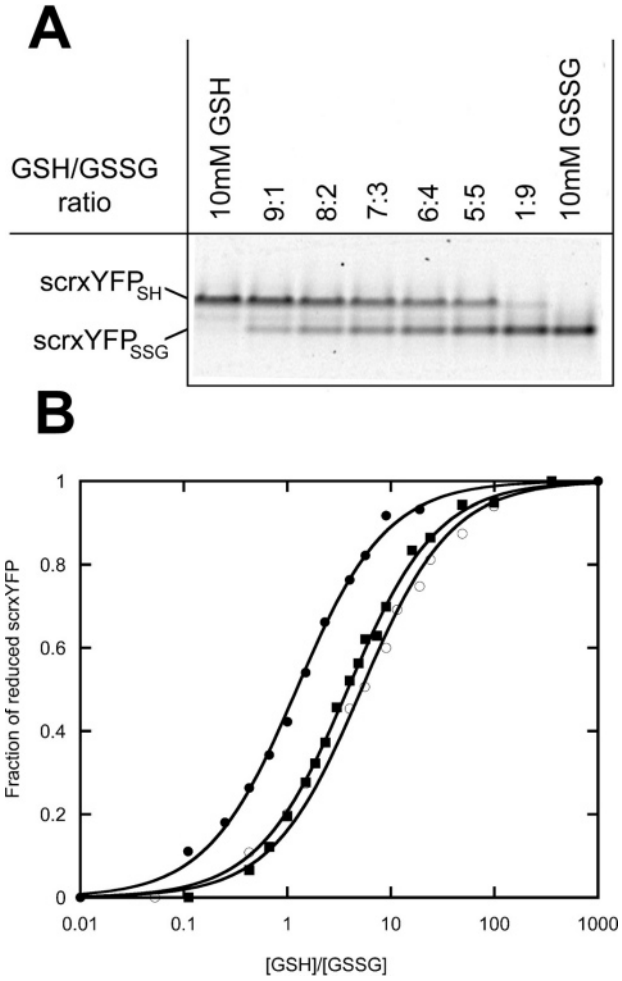

FIGURE 7: Determination of K_{scox}. (A) Following equilibration of scrxYFP$^{200R}_{149C}$ in buffers with varying GSH/GSSG ratios at pH 7.0 and 30 °C, samples were quenched with IAM and analyzed by nondenaturing gel electrophoresis to quantify unmodified (scrxYFP$_{SH}$) and glutathionylated protein (scrxYFP$_{SSG}$). (B) Redox titration curves of wt scrxYFP$_{149C}$ (○), scrxYFP$^{227R}_{149C}$ (■), and scrxYFP$^{200R}_{149C}$ (●) with reduced and oxidized glutathione. Equilibration of scrxYFP variants in buffers with varying [GSH]/[GSSG] ratios were carried out as described in A. K_{scox} values are given in the text.

DISCUSSION

We have used an artificial disulfide bond engineered into the yellow fluorescent protein (rxYFP) to study the reactivity and specificity of thiol−disulfide reactions. There are two aspects of this system that make it unique for these investigations: (a) the dithiol−disulfide pair is located on the rigid surface of the protein, and (b) the reduction and oxidation of the disulfide bond can easily be followed in real time by the change in fluorescence of the YFP scaffold. We have investigated how the reactivity and specificity of dithiol−disulfide exchange reactions are affected by modifying the electrostatic environment. We introduced positive charges in the vicinity of the disulfide bond to test the effect on the reactivity of rxYFP. Three solvent-exposed residues, Tyr200, Gln204, and Ala227, appeared to be suitable candidates for replacement with a positively charged residue. The initial experiments showed that both lysine and arginine substitutions increased the reactivity of the respective rxYFP forms. However, in all cases, the effects were more pronounced with arginine. Although the difference may be fortuitous, it may also reflect the fact that the positive charge is distributed over a larger volume in arginine and therefore is more likely to affect the pK_a of nearby titratable side chains. There is a clear inverse correlation between the rate enhancements in the single mutants and the distance from the inserted charge to the cysteine residues (Figures 2 and 4). If the contributions to rate enhancement were completely independent, it would be expected that the rate of the double mutant relative to the wt would be equal to the product of the relative rates of the single mutants (*19*, *20*). Not surprisingly, a comparison of the effects of double mutants with those of the single mutants shows that the mutual independence decreases with proximity. Interestingly, the 204R 227R double mutant was expected to give a 5.3-fold increase in the rate of oxidation with GSSG. The measured value of 5.4-fold is consistent with the fact that these residues are the most distant of the three mutated residues (13.6 Å for the C_α carbons). On the other hand, the 200 and 227 positions, which are at a distance of 4.9 Å for the C_α carbons, have predicted versus measured rate enhancements of 12.7 and 8.1, respectively. This trend is also found for HED as an oxidant. While the 13-fold increase in reactivity toward glutathione for the triple rxYFP$^{200R/204R/227R}$ mutant (Figure 4B) is substantial, it is far from the theoretical 22-fold that is predicted if the effects of positive charges were completely independent.

Much of the increased reactivity is due to specific electrostatic interactions with GSSG, as seen by the much less pronounced enhancements of activity toward HED and cysteamine disulfide. Similar investigations of electrostatic effects on the reactivity of cysteine thiols in peptides have previously been carried out (*6*, *21*). Introduction of three positive charges in the peptide Ac−YGGCAASQNN-NH_2, obtaining Ac−YGGCRAKRNN−NH_2, increased the reactivity toward HED by a factor of 1.7 and GSSG by a factor of 3.5, while pK_a dropped from 8.45 to 8.00 (*6*).

Reduced rxYFP is oxidized by GSSG with a rate constant in the same order of magnitude as the reaction of DTT with GSSG [72 and 180 M^{-1} min^{-1}, respectively (*22*)]. The 13-fold increase in reactivity observed for the triple-arginine mutant of rxYFP, compared to the 3.5-fold increase seen in the peptide, might be explained by a higher effective concentration of charge in rxYFP because of the smaller conformational flexibility of amino acid side chains in proteins compared to peptides. The importance of electrostatic interactions between the rxYFP mutants and negatively charged reagents was confirmed by comparing the reactions between negatively charged IAA or neutral IAM and the single-cysteine variants of wt rxYFP and rxYFP^{200R}, respectively. These experiments showed that the 200R mutation increased the reactivity at pH 9 toward IAA by 11.9-fold (Figure 6), whereas IAM reactivity only increased by 1.7-fold. The single-cysteine variants were also used to determine the pK_a values of the individual redox-active thiols as described previously for various oxidoreductases (*14*, *23*, *24*). From the pK_a determinations, it could be concluded that Cys149 was the predominant nucleophile with a pK_a of 8.9. A similar value of 8.7 has been determined for GSH (*17*) and is consistent with the observation that k_{app} for the reaction between DTT and oxidized rxYFP is close to the k_{app} for the reaction between DTT and oxidized glutathione (*7*). Interestingly, the pK_a values of GSH and Cys149 in rxYFP

are low compared to the thiol pK_a of, for example, DTT (pK_a = 9.2) and 2-mercaptoethanol (pK_a = 9.6). It appears that cysteines in peptides may have lower pK_a values than thiols in non-peptide compounds (*6*).

To determine whether introduction of positive charges affected the acidity of the predominant nucleophile, the pK_a values of Cys149 in wt rxYFP and rxYFP^{200R} were compared. This showed that the introduction of an arginine residue at position 200 resulted in a decrease in the pK_a of Cys149 by 0.7 units.

Determination of the equilibrium constants, K_{scox}, for the reaction between different scrxYFP$_{C149}$ variants and GSSG showed a decrease for the two scrxYFP mutants, scrxYFP$^{227R}_{149C}$ and scrxYFP$^{200R}_{149C}$. This confirmed that introduction of positive charges results in a stabilization of Cys149 thiolate in the rxYFP arginine variants (Figure 7). The stabilization of Cys149 as a leaving group appears to have a stronger effect than the putative electrostatic interaction between the introduced Arg residues and the negative charges on glutathione in the mixed disulfide. In general, the K_{scox} values were close to the ones previously determined for glutathionylation of protein thiols, where an average value of 1 has been reported (*25*, *26*). Interestingly, while all rxYFP variants had considerably increased reactivities toward glutathione, only two mutants had a significant change in the equilibrium constant, K_{ox} (where $K_{ox} = [rxYFP_{ox}][GSH]^2/[rxYFP_{red}][GSSG]$). The K_{ox} value of rxYFP^{200R} was decreased by a factor of 1.7 compared to that of the wt, while the K_{ox} value of rxYFP^{227R} was increased by 2.6-fold (data not shown).

Redox-sensitive forms of GFP provide very powerful tools for detailed analysis of factors affecting the reactivity and other redox properties of vicinal dithiols. Not only can the reactions be followed easily in the fluorimeter, in principle, the combination of nondenaturing gel electrophoresis with fluorescence scanning allows direct assessment of chemical modifications. We would note that this technique also allows for distinction and quantification of YFP forms in nonpurified samples. For example, it has the potential for quantitative determination of proteolytic cleavage events, phosphorylation, or other post-translational modifications in cell extracts without the need for subsequent immunostaining. In conclusion, the presented work has shown that, while reactivity of thiols in broad terms is determined by pK_a, accommodating for the charge properties of the reactants in specific cases may be of even greater importance.

ACKNOWLEDGMENT

We thank Olof Björnberg for help and advice in all aspects of this work. Morten Kielland-Brandt and Christine Tachibana are thanked for critically reading the manuscript. An anonymous reviewer is thanked for very constructive suggestions and corrections.

REFERENCES

1. Aslund, F., and Beckwith, J. (1999) The thioredoxin superfamily: Redundancy, specificity, and gray-area genomics, *J. Bacteriol. 181*, 1375−1379.
2. Martin, J. L. (1995) Thioredoxin—A fold for all reasons, *Structure 3*, 245−250.
3. Huber-Wunderlich, M., and Glockshuber, R. (1998) A single dipeptide sequence modulates the redox properties of a whole enzyme family. *Folding Des. 3*, 161−171.
4. Jacobi, A., Huber-Wunderlich, M., Hennecke, J., and Glockshuber, R. (1997) Elimination of all charged residues in the vicinity of the active-site helix of the disulfide oxidoreductase DsbA. Influence of electrostatic interactions on stability and redox properties. *J. Biol. Chem. 272*, 21692−21699.
5. Mossner, E., Huber-Wunderlich, M., and Glockshuber, R. (1998) Characterization of *Escherichia coli* thioredoxin variants mimicking the active-sites of other thiol/disulfide oxidoreductases, *Protein Sci. 7*, 1233−1244.
6. Bulaj, G., Kortemme, T., and Goldenberg, D. P. (1998) Ionization-reactivity relationships for cysteine thiols in polypeptides, *Biochemistry 37*, 8965−8972.
7. Ostergaard, H., Henriksen, A., Hansen, F. G., and Winther, J. R. (2001) Shedding light on disulfide bond formation: Engineering a redox switch in green fluorescent protein, *EMBO J. 20*, 5853−5862.
8. Fernandes, P. A., and Ramos, M. J. (2004) Theoretical insights into the mechanism for thiol/disulfide exchange, *Chem.—Eur. J. 10*, 257−266.
9. Sambrook, J., Fritsch, E. F., and Manaitis, T. (1989). *Molecular Cloning: A Laboratory Manual*, 2nd ed. Cold Spring Harbor Laboratory Press, Cold Spring Harbor, New York.
10. Topell, S., Hennecke, J., and Glockshuber, R. (1999) Circularly permuted variants of the green fluorescent protein, *FEBS Lett. 457*, 283−289.
11. Riddles, P. W., Blakeley, R. L., and Zerner, B. (1979) Ellman's reagent: 5,5′-Dithiobis(2-nitrobenzoic acid)—A reexamination, *Anal. Biochem. 94*, 75−81.
12. Chau, M. H., and Nelson, J. W. (1991) Direct measurement of the equilibrium between glutathione and dithiothreitol by high-performance liquid chromatography, *FEBS Lett. 291*, 296−298.
13. Ostergaard, H., Tachibana, C., and Winther, J. R. (2004) Monitoring disulfide bond formation in the eukaryotic cytosol, *J. Cell Biol. 166*, 337−345.
14. Takahashi, N., and Creighton, T. E. (1996) On the reactivity and ionization of the active site cysteine residues of *Escherichia coli* thioredoxin, *Biochemistry 35*, 8342−8353.
15. Reckenfelderbäumer, N., and Krauth-Siegel, R. L. (2002) Catalytic properties, thiol p*K* value, and redox potential of *Trypanosoma brucei* Tryparedoxin, *J. Biol. Chem. 277*, 17548−17555.
16. Tamarit, J., Bellí, G., Cabiscol, E., Herrero, E., and Ros, J. (2003) Biochemical characterization of yeast mitochondrial Grx5 monothiol glutaredoxin, *J. Biol. Chem. 278*, 25745−25751.
17. Szajewski, R. P., and Whitesides, G. M. (1980) Rate constants and equilibrium constants for thiol−disulfide interchange reactions involving oxidized glutathione, *J. Am. Chem. Soc. 102*, 2011−2026.
18. Gilbert, H. F. (1990) Molecular and cellular aspects of thiol−disulfide exchange, *Adv. Enzymol. Relat. Areas Mol. Biol. 63*, 69−172.
19. Mildvan, A. S., Weber, D. J., and Kuliopulos, A. (1992) Quantitative interpretations of double mutations of enzymes, *Arch. Biochem. Biophys. 294*, 327−340.
20. Mildvan, A. S. (2004) Inverse thinking about double mutants of enzymes, *Biochemistry 43*, 14517−14520.
21. Lutolf, M. P., Tirelli, N., Cerritelli, S., Cavalli, L., and Hubbell, J. A. (2001) Systematic modulation of Michael-type reactivity of thiols through the use of charged amino acids, *Bioconjugate Chem. 12*, 1051−1056.
22. Rothwarf, D. M., and Scheraga, H. A. (1992) Equilibrium and kinetic constants for the thiol−disulfide interchange reaction between glutathione and dithiothreitol, *Proc. Natl. Acad. Sci. U.S.A. 89*, 7944−7948.
23. Darby, N. J., and Creighton, T. E. (1995) Characterization of the active site cysteine residues of the thioredoxin-like domains of protein disulfide isomerase, *Biochemistry 34*, 16770−16780.
24. Nelson, J. W., and Creighton, T. E. (1994) Reactivity and ionization of the active site cysteine residues of DsbA, a protein required for disulfide bond formation *in vivo*, *Biochemistry 33*, 5974−5983.
25. Gilbert, H. F. (1995) Thiol/disulfide exchange equilibria and disulfide bond stability, *Methods Enzymol. 251*, 8−28.
26. Keire, D. A., Strauss, E., Guo W., Noszál, B., and Rabenstein, D. L. (1992) Kinetics and equilibria of thiol/disulfide interchange reactions of selected biological thiols and related molecules with oxidized glutathione, *J. Org. Chem. 57*, 123−127.

BI0500372